Open-loop Control for Permanent Magnet Synchronous Motor Driven by Square-wave Voltage and Stabilization Control

Daisuke Sato
Department of Electrical Engineering
Nagaoka University of Technology
Nagaoka, Niigata, Japan
dsato@stn.nagaokaut.ac.jp

Jun-ichi Itoh
Department of Electrical Engineering
Nagaoka University of Technology
Nagaoka, Niigata, Japan
itoh@vos.nagaokaut.ac.jp

***Abstract*— In this paper, the open-loop control for permanent magnet synchronous motor (PMSM) driven by a square-wave voltage is proposed. The proposed control is able to transit from the PWM region to the square-wave voltage region via the over modulation region seamlessly. When the PMSM is driven by the square-wave voltage using the proposed control, the low-frequency torque vibration except 6th or 12th order harmonics occurs due to the transition to the square-wave voltage region. Therefore, a variable band pass filter (BPF) is introduced as the reduction method of the low-frequency torque vibration. The low-frequency component in the active current for the stabilization control is extracted by the filter. As an experimental result, the proposed method reduces the low-frequency vibration which can be represented for the torque by over 40%.**

Keywords—Permanent magnet synchronous motor; Square-wave voltage; Open-loop control; Low-frequency torque vibration

I. INTRODUCTION

Recently, adjustable speed drive systems with a permanent magnet synchronous motor have been actively studied [1-5]. A voltage source inverter is applied to the drive systems widely, whereas the PMSM is driven by the PWM voltage, the over modulation voltage or the square-wave voltage. In addition, the PMSM is typically controlled by a field oriented control. However, it is difficult to control the PMSM by the typical field oriented control in the over modulation region and the square-wave voltage region because the controller becomes instable due to the harmonic currents [6]. Therefore, the control strategies in the over modulation region and the square-wave voltage region have been proposed, respectively [7-8]. The harmonic component is removed from the detected current by a low pass filter in order to implement a current feedback control in the over modulation region [7]. On the other hand, the torque is controlled by adjusting the voltage phase in the square-wave voltage region [8]. However, the switchover of the controller is necessary according to each voltage region. Therefore, the implementation of the controller becomes complex and the stability of the system is difficult to design.

In addition, it is proposed that the harmonic current is estimated from the motor and the inverter parameters used for a position sensorless control in order to implement the current feedback control in the over modulation region [9]. This control is able to be applied into both the PWM region and the over modulation region. However, the operation is not considered in the square-wave voltage region. Furthermore, the instantaneous current control in the square-wave voltage region has been proposed [10]. This control method is also applied to both the PWM region and the over modulation region. Therefore, the switchover of the controller is not necessary, although a field-programmable gate array (FPGA) is required in order to apply a space vector modulation to the inverter. The inverter is required to switch every 180 degrees in order to generate the square-wave voltage. Therefore, the FPGA which operates in several MHz is required. In other words, it is impossible to switch every 180 degrees accuracy only by the single-chip microcomputer which generates PWM based on triangular-wave comparison method. Therefore, the error in the inverter output voltage occurs. As a result, low-frequency torque vibration except 6th or 12th order harmonics occurs in the square-wave voltage region.

This paper proposes a control strategy for the PMSM based on the open-loop control implemented into the single-chip microcomputer, the control period of which is constant. The proposed method is able to transit from the PWM region to the square-wave voltage region via the over modulation region seamlessly. In particular, V/f control implemented with the stabilization control is applied in both the PWM region and the over modulation region [11-12]. In the square-wave voltage region, only the frequency is controlled. In principle, the torque includes the ripple, the frequency of which is six times the fundamental frequency. However, an additional lower order harmonic component also occurs in the square-wave voltage region, which fluctuates the torque. Hence, a reduction method of this low-frequency torque vibration is necessary. Therefore, a variable BPF is introduced. It extracts the low-frequency component from the active current for the stabilization control. This method reduces the low-frequency torque vibration without an additional sensor. First, this paper presents the characteristic of the open-loop control for the PMSM. Then, the operation verification of the PMSM is simulated in the square-wave voltage region. Next, the cause of the torque fluctuation is clarified and the low-frequency torque-vibration reduction

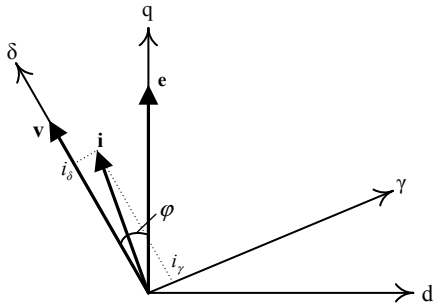

Fig. 1 Relationship between d-q coordinate and γ–δ coordinate. i_δ is active current and i_γ is reactive current.

method is proposed. Finally, the proposed method is verified by the simulation and the experiment.

II. Open-Loop Control of PMSM

A. Square-wave Voltage Drive by Open-loop Control

Generally, the direction of the flux in the permanent magnet is defined as d-axis and the direction of the back electromotive force is defined as q-axis in the field oriented control of the PMSM. However, d-q coordinate is not able to be defined in the open-loop control because the position of the magnetic pole is unknown. Therefore, the direction of the inverter output voltage is defined as δ-axis, whereas the axis which lags by π/2 rad from δ-axis can be defined as γ-axis in the open-loop control system.

Fig. 1 shows the relationship between the d-q coordinate and the γ–δ coordinate. The δ-axis component of the current vector i_δ expresses the active current because the δ-axis aligns in the same direction of the output voltage vector. Similarly, the γ-axis component of the current vector i_γ expresses the reactive current.

Fig. 2 shows the control block diagram of the open-loop control with the stabilization control for the PMSM [11-12]. The PMSM is driven by the V/f control in the PWM region and the over modulation region. In particular, the relationship between the fundamental amplitude of the output voltage and the modulation index is nonlinear in the over modulation region. Hence, the transition control, the modulation index in which is corrected, is necessary [9, 12]. In addition, the voltage amplitude is constant and the frequency is controlled only in the square-wave voltage region. Furthermore, in case that the PMSM is driven by a simple open-loop control, the control system becomes instable due to the fluctuation of the load angle. Therefore, the active current i_δ is fed back in order to adjust the output frequency command ω^*. By this method, the control system becomes stable because the equivalent feedback of the load angle is realized [11].

Fig. 3 shows the triangular-wave comparison method in each voltage region. The amplitude of the modulating wave is smaller than that of the triangular-wave in the PWM region. On the other hand, the amplitude of the modulating wave becomes larger than that of the triangular-wave by the transition control in the over modulation region and the square-wave voltage region. Therefore, each voltage waveform is able to be generated by the triangular-wave comparison method.

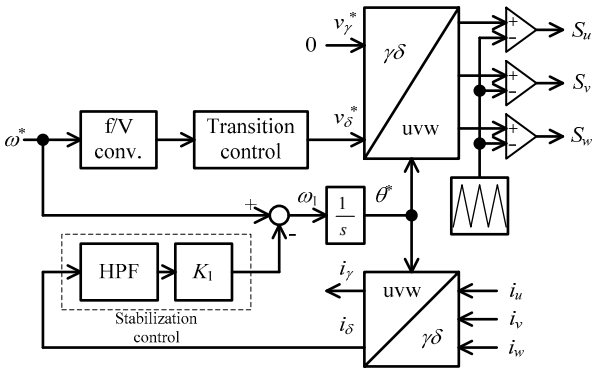

Fig. 2 Control block diagram of open-loop control with stabilization control for PMSM. The stabilization control is nesessary for the PMSM drive.

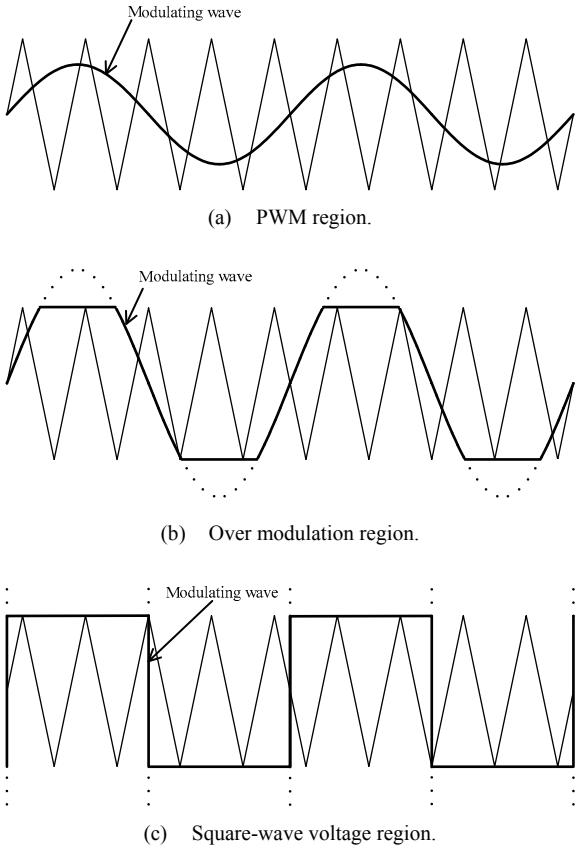

Fig. 3 Triangular-wave comparison method in each voltage region. The each voltage waveform is able to be generated by the triangular-wave comparison method.

Then, the PMSM is driven by the open-loop control and transited from the PWM region to the square-wave voltage region in simulation. The parameters of the PMSM in the simulation as well as the experiment are shown in Table 1. The two-level inverter, the carrier frequency of which is 10 kHz is applied in the simulation.

Fig. 4 shows the simulation results of the PMSM driven by the open-loop control. The speed is controlled smoothly from

the PWM region to the square-wave voltage region via the over modulation region. However, the torque fluctuation increases in particular speed of the square-wave voltage region.

Fig. 5 shows the torque harmonics analysis result at several points of speed in the square-wave voltage region. In principle, when the PMSM is driven by the square-wave voltage, the harmonic components, the orders of which are the multiples of six compared to the fundamental frequency occur in the torque. However, the lower order harmonic which is not the multiple of six also occurs. This significantly increases the torque fluctuation at ω = 0.74 p.u. and ω = 0.96 p.u. Because the excessive torque fluctuation worsens the speed response, the reduction of the low-frequency torque vibration is necessary.

B. *Analysis of Control System*

The cause of the increase in the low-frequency torque vibration is investigated. Therefore, the gain characteristics of the control system are obtained. In addition, the PMSM subjected to the analysis is a surface PMSM which the d-axis inductance equals to the q-axis inductance in order to simplify the analysis. First, the state equation and the output equation of the control system are obtained. The voltage of the PMSM on the γ–δ coordinate system is expressed in (1),

$$\begin{bmatrix} v_\gamma \\ v_\delta \end{bmatrix} = \begin{bmatrix} R+\dfrac{d}{dt}L & -\omega_1 L \\ \omega_1 L & R+\dfrac{d}{dt}L \end{bmatrix} \begin{bmatrix} i_\gamma \\ i_\delta \end{bmatrix} + \omega\psi_m \begin{bmatrix} \sin\varphi \\ \cos\varphi \end{bmatrix} \quad (1),$$

where v_γ is the γ-axis voltage, v_δ is the δ-axis voltage, R is the armature winding resistance, L is the armature inductance, ψ_m is the maximum value of armature linked flux, ω is the angular frequency of the PMSM, ω_1 is the angular frequency of inverter output and φ is the phase difference between the d-q coordinate and the γ-δ coordinate. Next, the torque is expressed in (2),

$$T = P_f \psi_m i_q = P_f \psi_m \left(i_\gamma \sin\varphi + i_\delta \cos\varphi \right) \quad (2),$$

where P_f is the number of the pole pairs and i_q is the q-axis current. In addition, the relationship between the angular frequency of the PMSM and the torque is expressed in (3).

$$\frac{d}{dt}\omega = \frac{P_f}{J}T \quad (3)$$

Furthermore, the rotational speed of the γ-δ coordinate is same as that of the d-q coordinate in the steady state. However, the rotational speed of two coordinates is varied by changing the rotational speed and the stability control in the transient state. Therefore, the differential of the phase difference is derived as in (4),

TABLE I. PARAMETERS OF THE PMSM

Rated power	3 kW
Rated torque	8 Nm
Maximum speed	12000 min^{-1}
Rated current	17.3 Arms
Pole number	4
d-axis inductance	2.04 mH
q-axis inductance	2.24 mH
Winding resistance	133 mΩ
Linked flux	0.1066 Vs/rad
Moment of inertia	0.0013 kgm^2

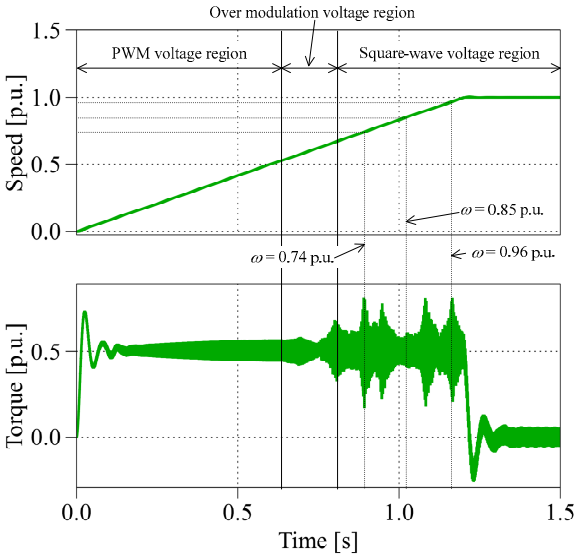

Fig. 4 Simulation results of PMSM driven by open-loop control. The torque fluctuation increases in the square-wave voltage region.

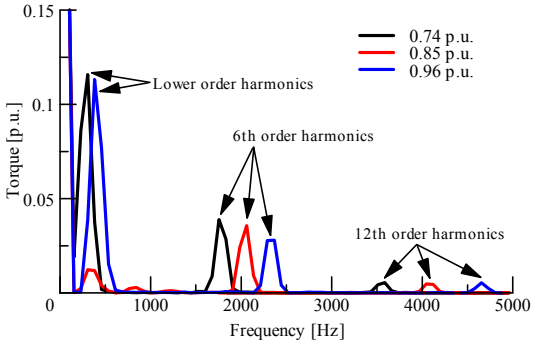

Fig. 5 Torque harmonics in square-wave voltage region. The lower order harmonic which is not the multiple of six also occurs.

$$\frac{d}{dt}\varphi = \omega_1 - \omega - K_1 i_\delta \qquad (4),$$

where K_1 is the gain of the stability control. In addition, the phase difference φ is same as the load angle by the definition of the γ-δ coordinate.

The open-loop control system is expressed as the fourth-order state equation by (1), (3) and (4). These equations are nonlinear. Therefore, these equations are linearized in the steady-state operating points. The state equation and the output equation after the linearization can be expressed in (5) and (6), respectively. Suffix '0' implies the values at the steady-state operating points. Then, the gain characteristics of the control system are obtained by (5) and (6). In addition, in order to evaluate the relationship between the gain characteristics and the speed of the PMSM, the gain characteristics are obtained at several different points of speed.

Fig. 6 shows the gain characteristics of the open-loop control for the PMSM. In the control system, these are three gain characteristics because the state equation has three input variables. However, $\Delta\omega_1$ is zero at the steady-state operating points. Therefore, only the gain characteristics of Δv_γ and Δv_δ are verified. From Fig. 6, it is understood that the control system has resonance frequency. The resonance frequency equals to the inverter output frequency. Hence, in case that Δv_γ and Δv_δ contain the resonance frequency component whose frequency is similar to the inverter output frequency, the low-frequency torque vibration increases.

The γ-axis voltage and the δ-axis voltage are fluctuated due to the transition to the square-wave voltage. In the square-wave voltage region, the control response becomes slow because the voltage changes only twice a period. Furthermore, the error of the voltage occurs because it is impossible to switch every 180 degrees by the single-chip microcomputer which generate the PWM based on triangular-wave comparison method. Therefore, the load angle easily fluctuates with the inverter output frequency which results in the fluctuation of the γδ-axis voltage. Consequently, the low-frequency torque vibration occurs and the δ-axis current which is fed back to the stabilization control also fluctuates. The fluctuation of the δ-axis current leads to the fluctuation of the γδ-axis voltage, which worsens the torque fluctuation.

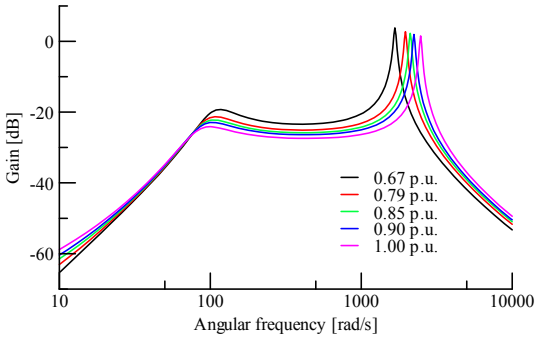

(a) Characteristic from Δv_γ to ΔT.

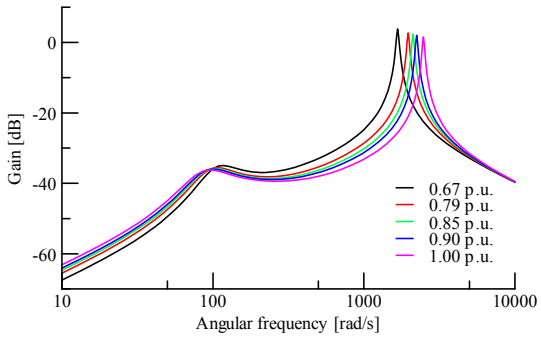

(b) Characteristic from Δv_δ to ΔT.

Fig. 6 Gain characteristics of open-loop control for PMSM. The control system has resonance frequency, which equals to the inverter output frequency.

III. Reduction Method of Low-Frequency Torque Vibration

The reduction method of the low-frequency torque vibration is considered. The low-frequency torque vibration increases

$$\frac{d}{dt}\begin{bmatrix}\Delta i_\gamma\\ \Delta i_\delta\\ \Delta\omega\\ \Delta\varphi\end{bmatrix} = \begin{bmatrix} -\frac{R}{L} & \omega_0 - K_1 i_{\delta 0} & -\frac{\psi_m}{L}\sin\delta_0 & -\frac{\psi_m}{L}\omega_0\cos\delta_0 \\ -\omega_0 & K_1 i_{\gamma 0} - \frac{R}{L} & -\frac{\psi_m}{L}\cos\delta_0 & \frac{\psi_m}{L}\omega_0\sin\delta_0 \\ \frac{{P_f}^2\psi_m}{J}\sin\delta_0 & \frac{{P_f}^2\psi_m}{J}\cos\delta_0 & 0 & \frac{{P_f}^2\psi_m}{J}\left(i_{\gamma 0}\cos\delta_0 - i_{\delta 0}\sin\delta_0\right) \\ 0 & -K_1 & -1 & 0 \end{bmatrix}\begin{bmatrix}\Delta i_\gamma\\ \Delta i_\delta\\ \Delta\omega\\ \Delta\varphi\end{bmatrix} + \begin{bmatrix} \frac{1}{L} & 0 & i_{\delta 0} \\ 0 & \frac{1}{L} & -i_{\gamma 0} \\ 0 & 0 & 0 \\ 0 & 0 & 1 \end{bmatrix}\begin{bmatrix}\Delta v_\gamma\\ \Delta v_\delta\\ \Delta\omega_1\end{bmatrix} \qquad (5)$$

$$\Delta T = \begin{bmatrix} P_f\psi_m\sin\varphi_0 & P_f\psi_m\cos\varphi_0 & 0 & P_f\psi_m\left(i_{\gamma 0}\cos\varphi_0 - i_{\delta 0}\sin\varphi_0\right)\end{bmatrix}\begin{bmatrix}\Delta i_\gamma\\ \Delta i_\delta\\ \Delta\omega\\ \Delta\varphi\end{bmatrix} \qquad (6)$$

because the γ-axis voltage and the δ-axis voltage are fluctuated by the transition to the square-wave voltage. Therefore, it is necessary to suppress the effect of the fluctuation of the δ-axis current for the drive system.

Fig. 7 shows the control block diagram of the open-loop control with the low-frequency torque vibration reduction control in the square-wave voltage region. The proposed control consists of the band pass filter (BPF). The resonance frequency component in the δ-axis current is extracted by the BPF. Then, it is fed back to adjust the inverter output frequency command. In addition, the mid-band frequency of the BPF is changed by the inverter output frequency command (variable BPF) because the resonance frequency of the control system changes according to the speed, i.e. the inverter output frequency. The variable BPF consists of the biquad filter. Furthermore, the proposed control is not necessary in the PWM region and the over modulation region. Therefore, the filter gain K_2 is zero in these regions.

Fig. 8 shows the block diagram of the variable biquad filter. The coefficients are varied by the inverter output frequency. In addition the biquad filter is expressed by (7),

$$y_n = b_0 u_n + b_1 z^{-1} u_n + b_2 z^{-2} u_n - a_1 z^{-1} y_n - a_2 z^{-2} y_n \quad (7),$$

where u_n is the input signal, y_n is the output signal and a_1, a_2, b_0, b_1 and b_2 are the coefficients. If the BPF consists of the biquad filter, the coefficients are expressed by (8) ~ (12),

$$a_1 = \frac{-2\cos\omega_c}{1+\alpha} \quad (8),$$

$$a_2 = \frac{1-\alpha}{1+\alpha} \quad (9),$$

$$b_0 = \frac{\alpha}{1+\alpha} \quad (10),$$

$$b_1 = 0 \quad (11),$$

$$b_2 = -\frac{\alpha}{1+\alpha} = -b_0 \quad (12),$$

where

$$\omega_c = \frac{2\pi f_c}{f_s} \quad (13),$$

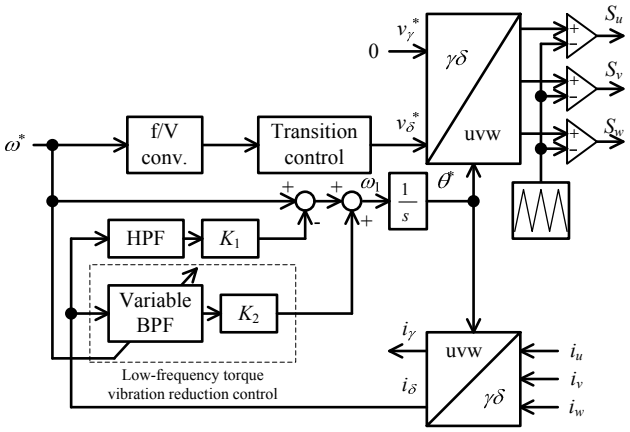

Fig. 7 Control block diagram of open-loop control with low-frequency torque vibration reduction control in square-wave voltage region. The reduction control is consist of the valiable BPF.

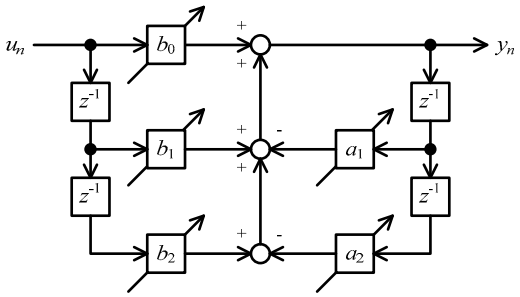

Fig. 8 Block diagram of variable biquad filter. The coefficients are varied by the inverter output frequency.

$$\alpha = \frac{\sin\omega_c}{2Q} \quad (14).$$

f_c is the center frequency, f_s is the sampling frequency and Q is Q factor. In this case, only a_1, a_2 and b_0 is calculated due to b_1 = 0 and b_2 = -b_0. In addition, the coefficients are changed by the center frequency.

Fig. 9 shows the coefficient characteristics of the BPF on the biquad filter. The sampling frequency is 10 kHz and Q factor is 0.7. The all coefficients are proportional to the center frequency, i.e., the coefficients are expressed by the linear equation. Therefore, the memory usage of the controller is not large.

Fig. 10 shows the simulation result of the PMSM drive by the open-loop control with the low-frequency torque vibration reduction control. The simulation condition is same as Fig. 3. It is confirmed that the fluctuation of the torque is reduced by the proposed method in the square-wave voltage region.

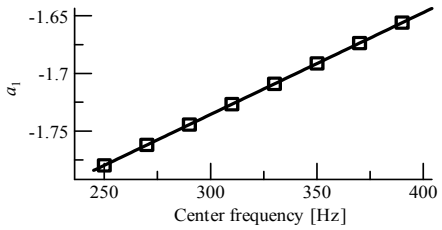

(a) a_1

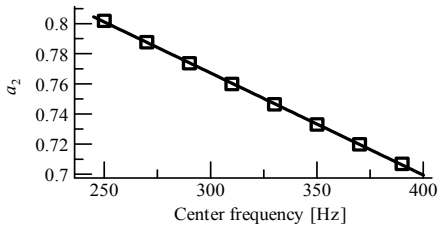

(b) a_2

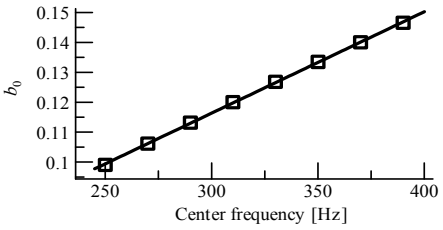

(c) b_0

Fig.9 Coefficient characteristics of band pass filter on biquad filter. The all coefficients are proportional to the center frequency.

Fig. 11 shows the torque harmonics when the low-frequency torque vibration reduction control is applied. The six-order component and 12-order component do not change compared to Fig. 4. On the other hand, the lower order component is reduced. Therefore, the stabilization of the torque is can be achieved.

Fig. 12 shows the comparison of the low-frequency torque vibration. The low-frequency torque vibration decreases by approximately 70% at the speed when the torque fluctuation becomes large (ω = 0.74 p.u. and ω = 0.96 p.u.). However, the low-frequency torque vibration is not removed completely because of the delay of the control response with the square-wave voltage as explained above.

IV. Experimental Result

In this section, the proposed control is verification by the experiment. The control period is 50 μs, whereas the variable B PF is consist of two-order IIR filter. In addition, the parameter of the PMSM in the experiment is shown in Table 1.

Fig. 13 shows the waveform of the line-to-line voltage and the phase current. The motor speed is 1.0 p.u. From Fig. 13, it is

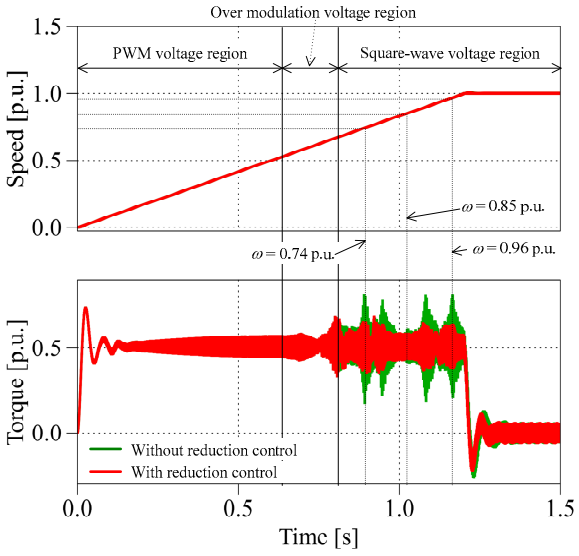

Fig. 10 Simulation result of PMSM drive by open-loop control with low-frequency torque vibration reduction control. The fluctuation of the torque is reduced by the reduction method.

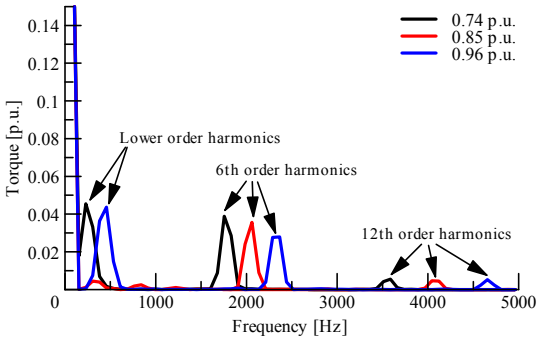

Fig. 11 Torque harmonics with low-frequency torque vibration reduction control. The lower order component is reduced compared to Fig. 4.

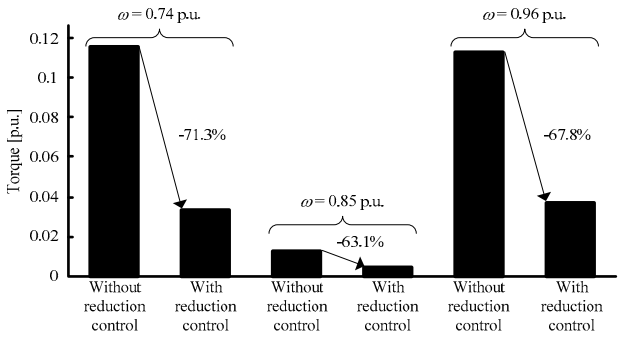

Fig. 12 Comparison of low-frequency torque vibration. The low-frequency torque vibration decreases by approximately 70% at the speed when the torque fluctuation becomes large (0.74 p.u. and 0.96 p.u.).

confirmed that the inverter is driven by the proposed control method in the square-wave voltage region.

Fig. 14 shows the waveform of the speed and the q-axis current when the PMSM is accelerated. In this experiment, it is difficult to measure the torque waveform directly. Therefore, the q-axis current is evaluated instead of the torque. In addition, the pole position is detected by the position sensor only in order to calculate the q-axis current. The controller does not use the position sensor. Furthermore, the acceleration time is 6.67 s from $\omega = 0.6$ p.u. to 1.0 p.u. because the torque fluctuation is likely to have a negative effect on the drive system when the motor is accelerated slowly. From Fig. 9(a), it is understood that the fluctuation of the q-axis current increases at several points of speed in the square-wave voltage region. On the other hand, in Fig. 9(b), the fluctuation of the q-axis current is reduced by the proposed control.

Fig. 15 shows the waveform of the speed and the q-axis current at $\omega_m = 0.943$ p.u. The fluctuation of the q-axis current also occurs in the steady state as with the accelerating. Moreover, the fluctuation component of the q-axis current is 0.325 p.u. without the low-frequency torque vibration reduction control. If the proposed control is applied, the fluctuation component is improved to 0.172 p.u.

Fig. 16 shows the comparison of lower order harmonic of the q-axis current. The speed to compare are 0.848 p.u., 0.908 p.u. and 0.943 p.u. At any compared speed, the fluctuation of q-axis current is large in Fig. 9. From Fig. 10, the lower order harmonic component of the q-axis current decrease by over 40% at any compared speed.

V. Conclusion

In this paper, the control strategy for the PMSM based on the open-loop control in the single-chip microcomputer is proposed. The proposed method is able to transit from the PWM region to the square-wave voltage region via the over modulation region seamlessly. In addition, the low-frequency torque vibration except 6th or 12th order harmonics occurs because the voltage is fluctuated by the transition to the square-wave voltage. Therefore, the low-frequency torque vibration reduction control using the variable BPF is proposed. As an experimental result, the low-frequency vibration decreases by over 40%.

References

[1] R. Tanabe and K. Akatsu, "Advanced Torque and Current Control Techniques for PMSMs with a Real-time Simulator Installed Behavior Motor Model", *IEEJ Journal of Industry Applications*, Vol.5, No.2, pp.167-173 (2016)

[2] X. Ji and T. Noguchi, "Online q-axis Inductance Identification of IPM Synchronous Motor Based on Relationship between Its Parameter Mismatch and Current", *IEEJ Journal of Industry Applications*, Vol.4, No.6, pp.730-731 (2015)

[3] T. Zanma, M. Kawasaki, K. Liu, M. Hagino, and A. Imura, "Model Predictive Direct Torque Control for PMSM with Discrete Voltage Vectors", *IEEJ Journal of Industry Applications*, Vol.3, No.2, pp.121-130 (2014)

[4] K. Ueda, S. Morimoto, Y. Inoue, and M. Sanada, "A Novel Control Method in Flux-weakening Region for Efficient Operation of Interior Permanent Magnet Synchronous Motor", *IEEJ Journal of Industry Applications*, Vol.4, No.5, pp.619-625 (2015)

[5] T. Yamaguchi, Y. Tadano, and N. Hoshi, "Using a Periodic Disturbance Observer for a Motor Drive to Dompensate Current Measurement Errors", *IEEJ Journal of Industry Applications*, Vol.4, No.4, pp.323-330 (2015)

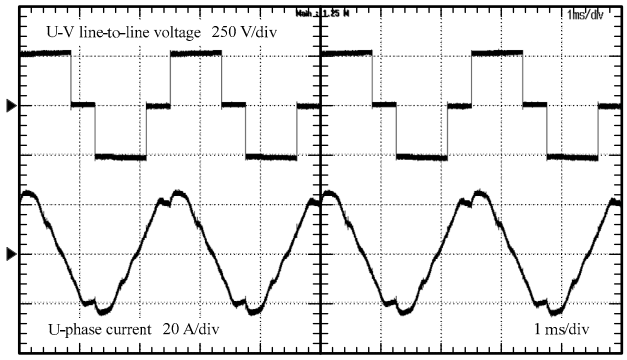

Fig.13 Waveform of line-to-line voltage and phase current in the square-wave voltage region. The motor speed is 1.0 p.u.

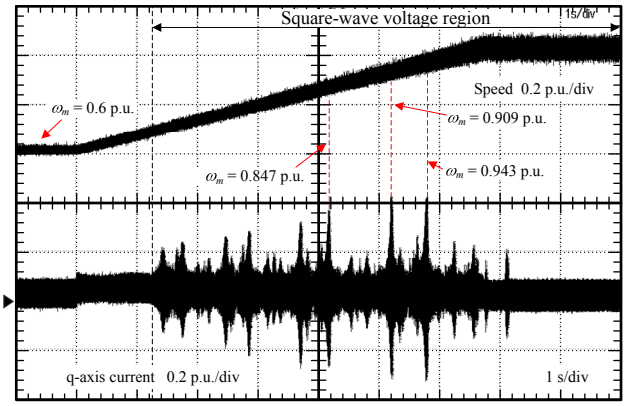

(a) Without low-frequency torque vibration reduction control. The fluctuation of the q-axis current increases at several points of speed in the square-wave voltage region.

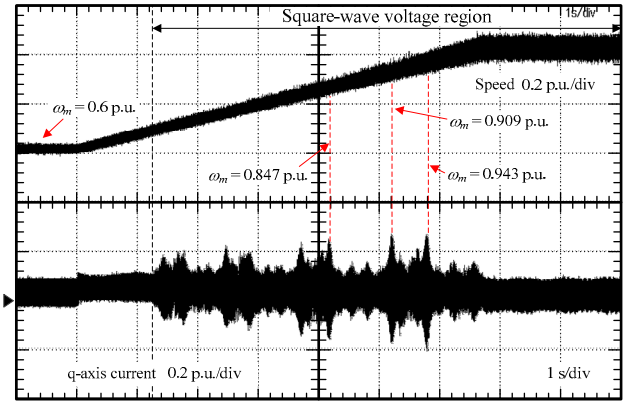

(b) With low-frequency torque vibration reduction control. The fluctuation of the q-axis current is reduced by the proposed control.

Fig. 14 Waveform of motor speed and q-axis current. The q-axis current is evaluated instead of the torque.

[6] A. M. Khambadkone and J. Holtz, "Compensated Synchronous PI Current Controller in Overmodulation Range and Six-Step Operation of Space-Vector-Modulation-Based Vector-Controlled Drives", *IEEE Trans of Ind. Electron.*, Vol.49, No.3, pp.574-580 (2002)

[7] H. Nakai, H. Ohtani, and Y. Inaguma, "Novel Torque Control Technique for High Efficiency/High Power Interior Per manent Magnet Synchronous Motors", R&D Review of Toyota CRDL, Vol.40, No.2, pp.44-49 (2005)

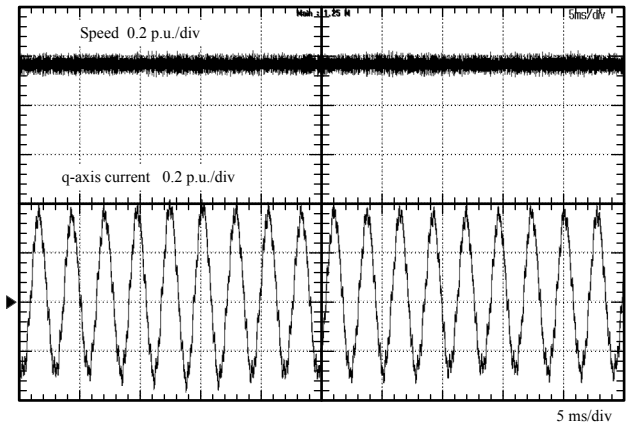

(a) Without low-frequency torque vibration reduction control.

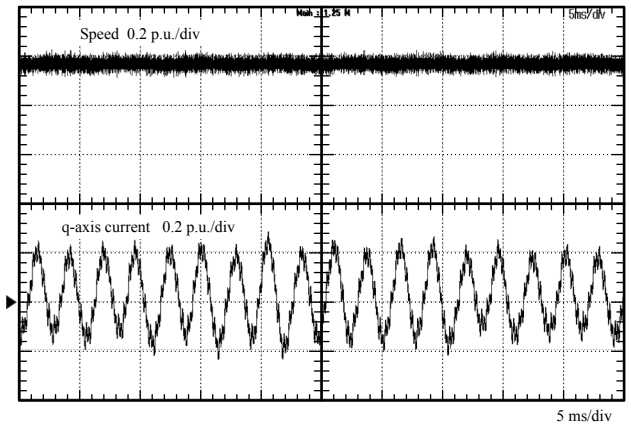

(b) With low-frequency torque vibration reduction control.

Fig. 15 Waveform of motor speed and q-axis current at ω_m = 0.943 p.u.

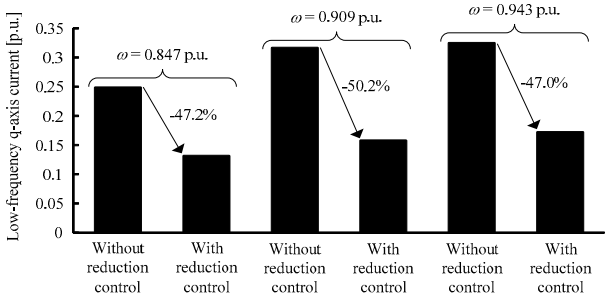

Fig. 16 Comparison of low-frequency q-axis current. The lower order harmonic component of the q-axis current decrease by over 40% at any compared speed.

[8] H. Nakai, H. Ohtani, E. Satoh, and Y. Inaguma, "Development and Testing of the Torque Control for the Permanent-Magnet Synchronous Motor", *IEEE Trans. Ind. Electron.*, Vol.52, No.3, pp.800-806 (2005)

[9] D. Asano, S. Lerdudomsak S. Doki, and S. Okuma, "Position Sensorless Torque Control System of PMSM in Overmodulation Range", IPEC2010, pp.1407-1411 (2010)

[10] Y. C. Kwon, S. Kim, and S. K. Sul, "Six-Step Operation of PMSM With Instantaneous Current Control", *IEEE Trans. Ind. Appl.*, Vol.50, No.4, pp.2614-2625 (2014)

[11] J. Itoh N. Nomura, and H. Ohsawa, "A comparison between V/f control and position-sensorless vector control for the permanent magnet synchronous motor", PCC2002, pp.1310-1315 (2002)

[12] J. Itoh and N. Ohtani, "Square-Wave Operation for a Single-Phase-PFC Three-Phase Motor Drive System Without a Reactor", *IEEE Trans. Ind. Appl.*, Vol.47, No.2, pp.805-811 (2011)